

# Beta Decay studies of neutron-rich nuclei around $N=40$

O. Sorlin

Institut de Physique Nucléaire, IN2P3-CNRS, F-91406 Orsay, France

$\beta$ -decay studies of neutron-rich nuclei at or around  $N=40$  are presented in the Co, Mn and V isotopic chains aiming to study excited states in Ni, Fe and Cr isotopes respectively. Examples are taken from experimental studies achieved at Louvain La Neuve, CERN/ISOLDE and GANIL/LISE facilities. Increases in production rates in the last five years has brought a dramatic change in the spectroscopic knowledge in this region of mass when the isospin number is increased. If the spherical  $N=40$  subshell is well-established for  $^{68}\text{Ni}$ , its effect is steadily decreased when proceeding towards  $^{64}\text{Cr}$  which lies at the mid-distance between  $Z=20$  and  $Z=28$  magic shells.

## 1. Introduction

Near the edge of stability, the surface of the neutron-rich nuclei would be essentially composed with a diffuse neutron-matter. The diffuseness should already be felt before the drip-line, for nuclei with large  $N/Z$  ratios. Theoretical calculations from HFB and RMF suggest that for such neutron-rich nuclei, a better description would be obtained with a more rounded potential that can be simulated by the harmonic oscillator potential [1]. The increase of the  $N=40$  subshell gap naturally arises from this approach. As a consequence, the well-pronounced shell-gap at  $N=50$  should be reduced. The  $^{68}\text{Ni}_{40}$  nucleus exhibits a high  $2^+$  energy of 2.033 MeV [2], in contrast to its neighbouring isotopes  $^{66}\text{Ni}$  and  $^{70}\text{Ni}$  whose  $2^+$  energies are 1425 keV [3] and 1259 keV [4], respectively. The sudden increase of the  $2^+$  energy at  $N=40$ , correlated to a sudden drop in  $B(E2)$  [5] suggests that  $^{68}\text{Ni}$  behaves like a magic nucleus. It has been shown with theoretical calculations that it can be considered as a good core to modelize nuclei in its vicinity [6]. However, the size of the energy gap at  $N=40$  in Ni has been proven to be of about 1 MeV by combined results in  $\beta$ -decay and isomer-decay studies (section 2). As a comparison, the  $N=20$  and  $N=28$  energy gaps are of 2.79MeV and 2.01MeV deduced from the level schemes of  $^{39}\text{Ca}$  and  $^{47}\text{Ca}$ , respectively. In order to determine whether a sizeable increase of this subshell-gap can be seen while increasing the isospin,  $\beta$ -decay studies has been extended to lighter- $Z$  isotones. Surprisingly, the removal of few protons from the  $^{68}\text{Ni}$  core significantly affects the structure of the nucleus which turns out to be quickly deformed. Experimental indications on this region of deformation south to  $^{68}\text{Ni}$  are given in the following with tentative hints to explain this phenomenon. It is obvious that, due to deformation, the observation of the predicted increase of the spherical  $N=40$  energy-gap is not possible in this region. Perspectives to reach this information are indicated in the conclusion.

## 2. Beta Decay of Co isotopes at Louvain La Neuve

Beta-decay of neutron-rich  $^{66-70}\text{Co}$  isotopes have provided a wealth of information concerning the structure of Ni isotopes around  $N=40$  [7–9]. These nuclei have been produced at the Louvain La Neuve facility in a 30MeV proton-induced fission reaction of a  $^{238}\text{U}$  target of  $15\text{mg}/\text{cm}^2$  thickness. The target was mounted in the Ar gas cell of the Leuven ion-guide laser-ion source (LIGLIS). The fission products were transported by the gas out to the exit hole of the cell where Co isotopes were selectively ionized by two lasers. The charged isotopes with a charge  $Q$  and mass  $A$  were subsequently separated in  $A/Q$  by the LISOL mass separator and guided to the detection point. The detection set up consisted of two high-purity Ge detectors (used for  $\gamma$ 's) and of three plastic detectors (used for  $\beta$ 's) arranged in a compact geometry.  $\beta$ - $\gamma$  and  $\gamma$ - $\gamma$  coincidences were required for the triggering of the acquisition system.

$\beta$ -decay of  $^{67}\text{Co}$  has been undertaken by Weissman et al. [7] who have measured a half-life of  $425(20)\text{ms}$ , in accordance with the results of [10–12]. About 92% of the  $\beta$ -decay occur via Gamow Teller transition to the  $5/2^-$  state in  $^{67}\text{Ni}$  at 694 keV whose spin-assignment was given by Pawlat et al. [3]. Three percent of the decay feed the  $9/2^+$  isomer [3,4] at 1007 keV by first forbidden transition type. The authors conclude that the measured half-life disagrees with all presently available calculations, which have however a good predictability in the neighbouring neutron-rich Ni isotopes [13]. This case of  $^{67}\text{Co}$  therefore remains a puzzle.

$\beta$ -decay of  $^{69}\text{Co}_{42}$  has been studied by Mueller et al. [8]. They have measured a half-life of  $220(20)\text{ms}$ , in agreement with the values of  $270(50)\text{ms}$  [14] and  $190(40)\text{ms}$  [12]. Part of the level-scheme of its decay is shown in Fig. 1 which contains the major ingredients that will be discussed in the following. This nucleus, of probable  $7/2^-$  configuration given by the proton hole in  $f_{7/2}$ , contains a pair of neutrons in  $g_{9/2}$ . In the  $\beta^-$ -decay of  $^{69}\text{Cu}$ , a neutron is converted to a proton which subsequently couple to the odd proton to form  $^{69}\text{Ni}$ . It is seen in the decay-scheme that the neutron is preferentially taken from the  $f_{5/2}$  orbital, keeping the two neutrons in  $g_{9/2}$  paired on. About 50% of the decay is feeding the  $5/2^-$  first state in  $^{69}\text{Ni}$ . This level deexcites by a 594 keV transition to a  $1/2^-$  state whose presence was first suggested by Grzywacz et al. [4]. This state due to a hole configuration in  $p_{1/2}$  corresponds to a rearrangement in the fp shell which cools down the nucleus. The detailed study of this  $1/2^-$   $\beta$ -decay isomer has been achieved by Mueller et al. [8] and by Prisciandaro et al. [11]. From these studies, it is found that 77% of the decay of this state occur to a  $3/2^-$  excited state at 1298 keV in  $^{69}\text{Cu}$ . The natural configuration of  $^{69}\text{Cu}$  corresponds to one proton of the  $2p_{3/2}$  orbital added to a  $^{68}\text{Ni}$  core. It is therefore expected that its g.s. configuration is  $3/2^-$  by coupling the extra-proton to the  $0^+$  core which is thought to be mainly given by a  $\nu(p_{1/2})^2$  configuration. The excited state at 1298 keV is expected to be due to the coupling of the extra-proton to the  $0_2^+$  core mainly given by  $\nu(g_{9/2})^2$  configuration. Since the  $1/2^-$  isomer in  $^{69}\text{Ni}$  decays preferentially through this excited  $3/2^-$ , this suggests that the  $g_{9/2}$  neutron-pair is still not broken in the decay. From this whole  $\beta$ -decay sequence,  $^{69}\text{Co} \rightarrow ^{69}\text{Ni} \rightarrow ^{69}\text{Cu}$ , it is fascinating to notice that the  $g_{9/2}$  neutron-pair is preferentially preserved. This effect is due to the strong pairing energy gained by coupling two neutrons in the  $g_{9/2}$  orbital. In order to evidence the impact of this high pairing energy, the authors of [8] noticed that the difference in energy between

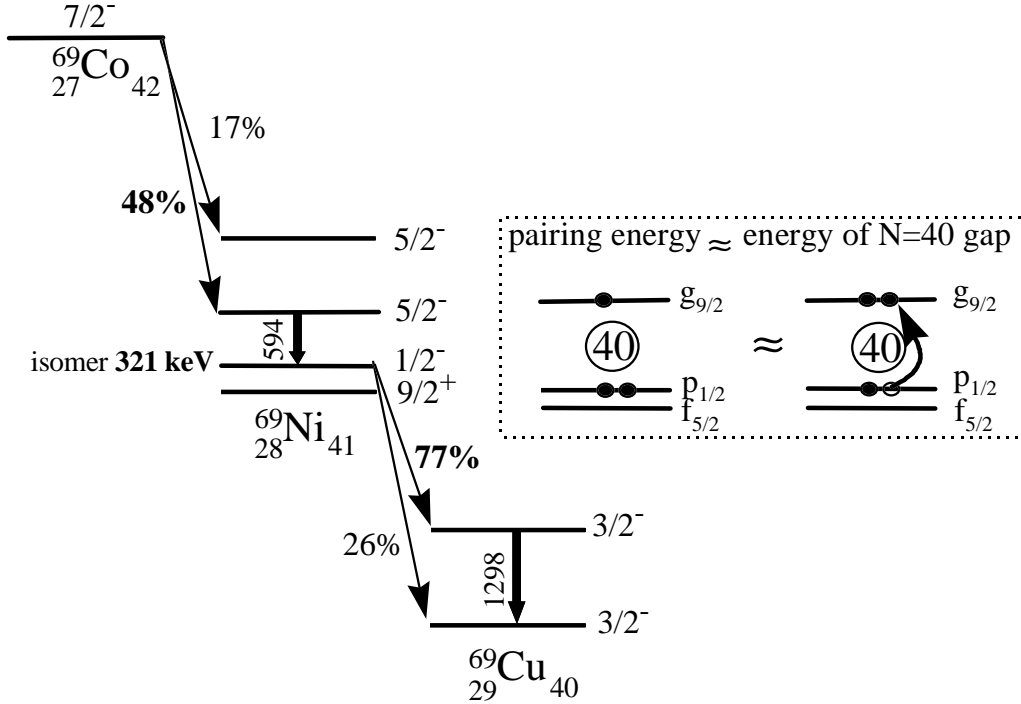


Figure 1. Partial  $\beta$ -decay scheme of  $^{69}\text{Co}$ .

the  $9/2^+$  and  $1/2^-$  states in  $^{69}\text{Ni}$  is only of 321 keV. The g.s. configuration corresponds to the natural feeding of a neutron in the  $g_{9/2}$  orbital, right above the  $N=40$  gap. The  $1/2^-$  configuration corresponds to the promotion of a neutron from the  $p_{1/2}$  orbital which subsequently couples to the single neutron in  $g_{9/2}$ . As a consequence, the energy of the  $N=40$  gap is 321 keV higher than the energy gained by coupling a pair of neutrons in  $g_{9/2}$  as compared to  $p_{1/2}$ . The size of the energy gap across  $N=40$  can be estimated to 1.007 MeV by the difference in single-particle levels  $p_{1/2}$  and  $g_{9/2}$  extracted from  $^{67}\text{Ni}$  [3].

### 3. Beta Decay studies of Mn isotopes at CERN

Neutron-rich Mn isotopes with masses up to  $A=69$  have been produced in spallation of uranium target of  $51 \text{ g/cm}^2$  thickness induced by 1 GeV protons of the CERN Proton Synchrotron Booster. Manganese isotopes have been extracted from the target after having been ionized by a chemically selective laser ion source. Mass-separated Mn isotopes have been transmitted to either a  $\beta$ -delayed neutron counter or to a two-HPGe  $\gamma$ -ray spectroscopy set-up. The counting time in each system was adjusted to the proton pulse beam of 1.0s duration separated by multiple of 1.2 seconds. Decay curves have been obtained by Hannawald et al. [15] with the  $\beta$ -neutron coincidence requirement.

New half-lives of 89(4), 88(4) and 66(4)ms have been determined for  $^{64}\text{Mn}$ ,  $^{65}\text{Mn}$  and  $^{66}\text{Mn}$  respectively. These values are in good accordance with the lately measured half-lives of [12] obtained at GANIL with a different method. With the use of the  $\gamma$ -ray

spectroscopy set-up,  $2^+$  energies of  $^{64}\text{Fe}$  (746keV) and  $^{66}\text{Fe}$  (573 keV) have been extracted from the  $\beta$ -decays of  $^{64}\text{Mn}$  and  $^{66}\text{Mn}$ . Contrary to the Ni isotopic chain, the Fe chain exhibits a sharp drop in  $2^+$  energies after reaching a maximum at  $^{62}\text{Fe}_{36}$  (Fig. 6). It is clear from the difference in  $2^+$  energy between  $^{68}\text{Ni}$  (2.003MeV) and  $^{66}\text{Fe}$  (573keV) that the removal of two protons from  $^{68}\text{Ni}$  has dramatically affected the structure of the core nucleus. The authors mention that the strong proton-neutron interaction between the two proton holes in  $f_{7/2}$  and the neutrons in  $g_{9/2}$  states is responsible for the lowering of the energy of spherical  $g_{9/2}$  orbital. With the lowering of this base orbital, downsloping levels as  $\nu[440]1/2^+$  or  $\nu[404]9/2^+$  (respectively prolate or oblate states) are more likely occupied than the spherical ones. This triggers deformation at  $N=40$ . This could be also viewed in the way that the proton core is less rigid when “wounded” by the removal of two protons. It could subsequently slightly be deformed. The large spacial recovering of proton ( $f_{7/2}$ ) and neutron ( $g_{9/2}$ ) orbitals, both of large orbital momentum, leads to a global modification of the nucleus. To get an idea on the deformation of  $^{66}\text{Fe}$ , Hannawald et al. [15] compare its  $2^+$ -energy (573keV) to those of  $^{72}\text{Zn}$  (652keV) and  $^{76}\text{Ge}$  (563keV). For these latter nuclei, deformation parameters of  $\beta_2=0.23$  [16] and 0.26 respectively [17], have been extracted from the measurement of their  $B(E2)$ . By extrapolating the  $2^+$ -energy deformation systematics to  $^{66}\text{Fe}$  with the empirical law obtained from [18,19]:

$$\beta_2 = cst \times \sqrt{A^{-0.69}/E(2^+)}, \quad (1)$$

they obtain a deformation parameter of  $\beta_2$  close to 0.26 [15].

## 4. Beta decay studies of V and Cr isotopes at GANIL

### 4.1. experimental procedure

The neutron-rich Ti-Co isotopes have been produced at GANIL by the fragmentation of a 60.4 A.MeV  $^{86}\text{Kr}^{34+}$  beam of 1.2 e $\mu$ A onto a  $^{58}\text{Ni}$  target with a thickness of 140  $\mu\text{m}$ . A carbon foil of 9.5 mg.cm $^{-2}$  was placed behind the production target to act as a stripper. Fragments of interest were separated by the LISE3 achromatic spectrometer. A wedge-shaped Be foil of 219  $\mu\text{m}$ -thickness was placed in the intermediate focal plane of the spectrometer in order to reduce the rate of nuclei close to stability. Two magnetic rigidity settings of the spectrometer were used to select nuclei with increasing neutron-richness. The nuclei transmitted in the higher magnetic rigidity setting are shown in Fig. 2. The selected nuclei were identified by means of 4 consecutive 300, 300, 500, 500  $\mu\text{m}$  silicon detectors placed close to the final focal plane of LISE3. They were implanted in the last detector divided in twelve 2 mm-wide, 24 mm-height vertical strips. In each strip, the energy and time for heavy ions as well as for the  $\beta$ -particles coming from their decay were measured. Each time a nucleus was implanted, the primary beam was switched off during 1.5 seconds to prevent the implantation of other nuclei which would act as  $\beta$ -contaminants. A  $\beta$ -event was considered as valid if occurring in the same strip #i as the precursor nucleus or in one of the neighbouring strips #i-1 and #i+1. The fitting procedure to determine the half-lives and the complete results obtained in the region of mass can be found in [12].

Five Ge detectors were placed in a cross geometry around the implantation detector for the detection of the main  $\gamma$  transitions. For instance, the strong  $\gamma$ -lines observed in

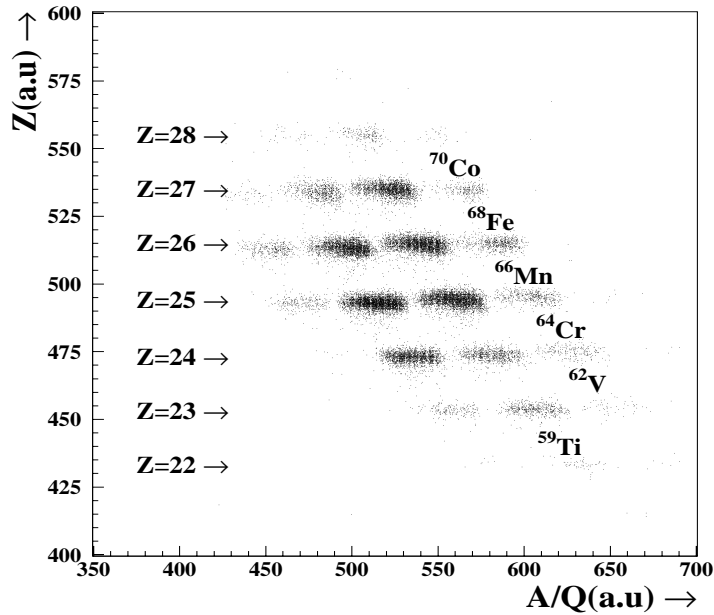


Figure 2. Identification of the nuclei produced in one of the setting of the spectrometer.

the decay of  $^{64}\text{Mn}$  and  $^{60}\text{V}$  have been attributed to the  $2^+ \rightarrow 0^+$  transitions in even-even nuclei  $^{64}\text{Fe}$  and  $^{60}\text{Cr}$ , respectively. Also, delayed  $\gamma$ 's in the 80- $\mu\text{s}$  time-range after the implantation of a nucleus have been observed. These  $\gamma$ 's characterize the presence of an isomer produced in the fragmentation process which survived along the 400 ns flight-time in the spectrometer. Isomeric transitions from excited states of  $^{59}\text{Cr}$ ,  $^{60}\text{V}$ ,  $^{64}\text{Mn}$  and  $^{67}\text{Fe}$  have been observed in agreement with the values reported in [4,20]. Their observation confirms the identification of the nuclei transmitted in the present experiment.

#### 4.2. results

Decay curves obtained in the V chain are shown in Fig. 3. For  $^{59}\text{V}$ , a half-life of 75(7)ms has been found. This half-life is in good accordance with the value of 70(40)ms [21], but not with the 130(20)ms obtained by Ameil et al. [22] with a smaller number of nuclei implanted and a higher beta-background. The  $\beta$ -decay of  $^{59}\text{V}$  of probable  $\pi f_{7/2}$  configuration mainly occurs through a pure Gamow-Teller transition to a  $\nu f_{5/2}$  state, which subsequently deexcites by emitting two  $\gamma$ -lines at 102(1) and 208(1) keV [12]. Due to beta-decay selection rules, the feeding of the  $\nu g_{9/2}$  isomer at 503(1) keV observed by Grzywacz et al. [4] in  $^{59}\text{Cr}$  is extremely hindered since it requires both a change of parity and of one unit in orbital momentum. The decay of this isomer, of 96(20) $\mu\text{s}$ , occurs by the emission of three  $\gamma$ 's of 102, 193 and 208 keV [4]. By comparing the two experiments, the isomeric transition can be clearly attributed to the  $\gamma$ -line at 193 keV, which is "missing" in the  $\beta$  decay. On the basis of energy and half-life of this transition, it is attributed to an M2 isomer. A tentative level scheme of  $^{59}\text{Cr}$  is drawn in the right part of Fig. 4.

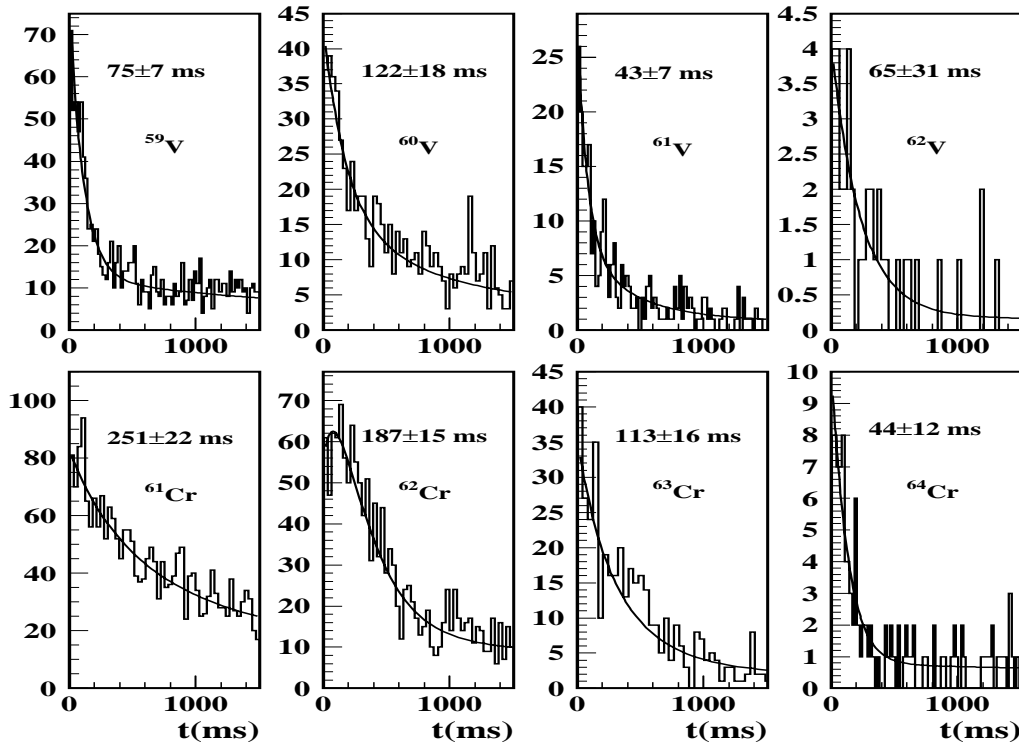


Figure 3. Decay curves of V and Cr isotopes. Numbers refer to half-lives.

It takes into account the experimental constraints from both isomer decay of  $^{59m}\text{Cr}$  and  $\beta$ -decay of  $^{59}\text{V}$ . This peculiar study shows the complementarity between the two methods to determine level scheme and assign spins of very exotic nuclei.

The presence of this  $9/2^+$  state so low in energy (503 keV above the g.s.) is surprising for a nucleus containing 35 neutrons, the “natural” feeding of this shell occurring in principle above 40 neutrons. As a comparison, this state is at 1065, 1291, and 861 keV in the isotones  $^{65}\text{Zn}$ ,  $^{63}\text{Ni}$ , and in the recently studied  $^{61}\text{Fe}$  [4] respectively. This decrease in energy of the  $g_{9/2}$  orbital with respect to the g.s. while making holes in  $^{68}\text{Ni}$  has been already suggested by Hannawald et al [15] for explaining the onset of deformation in  $^{66}\text{Fe}$  (see also the discussion in section 3). It is noticeable that the decrease in energy of this  $g_{9/2}$  orbital at  $N=35$  is strongly correlated with the decrease in the  $2^+$ -energy in even-even  $N=36$  nuclei, as illustrated in Fig. 5.

P. Möller [23] predicts that, in this Cr, V region of mass, the potential-energy surfaces are very soft with two shallow minima of different shapes separated by barriers of only 100 keV height. As an example, the ground state configuration of  $^{59}\text{V}$  is predicted to be prolate ( $\epsilon_2=0.15$ ) but the oblate minimum ( $\epsilon_2=-0.1$ ) is only 120 keV higher in energy. Similar shape-coexistence behaviour is found in the  $^{59}\text{Cr}$  daughter nucleus. In  $^{59}\text{Cr}$ , a prolate g.s. is expected ( $\epsilon_2=0.183$ ), the oblate configuration ( $\epsilon_2=-0.133$ ) is found 480 keV above. From the observed  $1/2^-$  g.s. configuration and the  $9/2^+$  isomer in  $^{59}\text{Cr}$  at a low energy of 503 keV, we can speculate that oblate shape is probably minimum in the

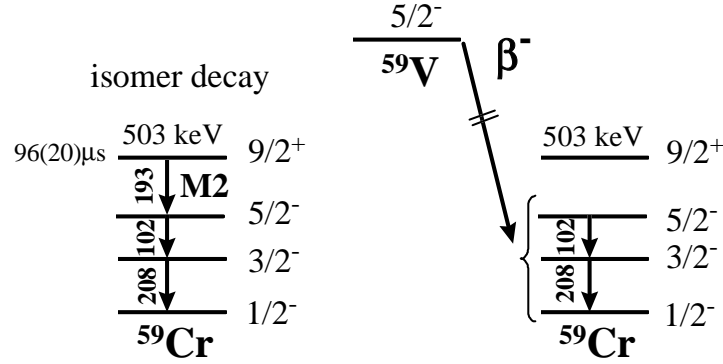


Figure 4. Left part :  $\gamma$ -lines obtained in  $^{59m}\text{Cr}$  decay, Right part : tentative beta-decay scheme of  $^{59}\text{Cr}$

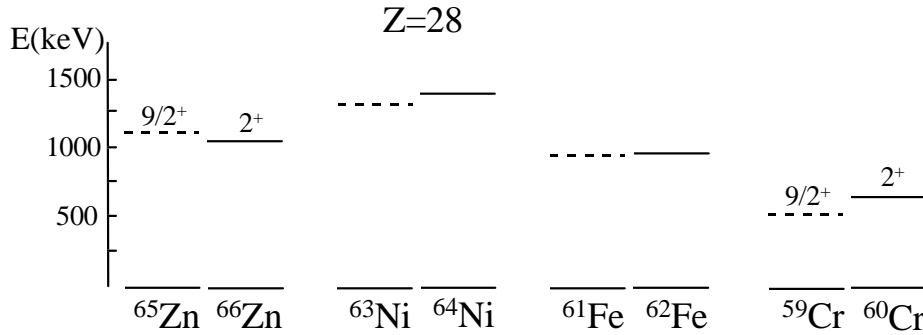


Figure 5. Energies of  $9/2^+$  and  $2^+$  states in  $N=35$  and  $N=36$  nuclei.

potential-energy surface of this nucleus. Indeed, the  $35^{\text{th}}$  neutron occupies a  $1/2^-$  shell for an oblate shape (see for instance the FY-levels single-neutron energies of fig. 7 of ref. [21] calculated for  $^{58}\text{V}$ ). Also, only in the case of an oblate shape, the down-sloping  $[404]9/2^+$  orbital is likely to be occupied by neutrons. The levels deduced in Fig. 4 beneath 503 keV could result from a mixture of prolate and oblate states. While moving to  $^{60}\text{Cr}$ , the g.s. configuration may have a large contribution of  $\nu(g_{9/2})^2$  configurations. In fact, the energy required to promote two neutrons in  $g_{9/2}$  (1.006 MeV) is very similar to the gain in pairing energy when coupling two neutrons in  $g_{9/2}$  as compared to  $p_{1/2}$  (1.3 MeV from [24]).

From the decay of  $^{60}\text{V}$ , of 122(18)ms half-life, a strong transition has been observed at 646(1) keV, corresponding probably to the  $2^+ \rightarrow 0^+$  transition in  $^{60}\text{Cr}$ . This  $2^+$  energy is much lower than that of the isotones  $^{66}\text{Zn}$ ,  $^{64}\text{Ni}$  and  $^{62}\text{Fe}$  at 1039, 1345 and 877 keV respectively (see Fig. 4,5). This energy decrease indicates that Cr nuclei develop more collectivity than Fe ones. This isotope resides at a half occupancy of  $\pi f_{7/2}$  shell, and the

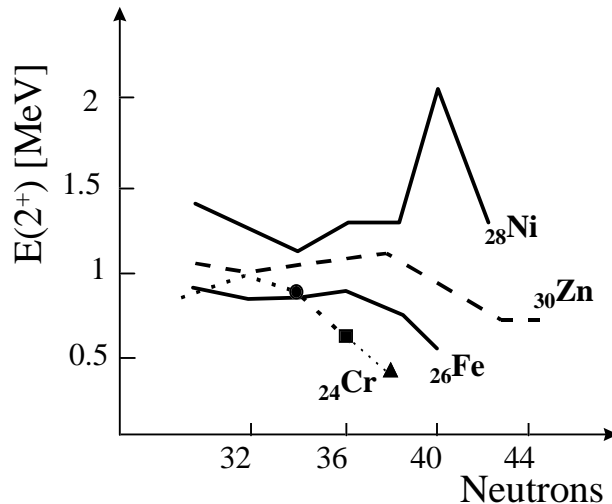


Figure 6.  $2^+$  energies in the Cr-Zn isotopic chains around  $N=40$ . Experimental values in Cr chain with filled circle and square are taken from Prisciandaro et al. [25] and [12] respectively. The  $2^+$  energy of  $^{62}\text{Cr}$  (filled triangle) is a preliminary value taken from a recent experiment performed at the GANIL facility.

four protons above  $Z=20$  are filling two downsloping orbitals in the Nilsson picture as the deformation parameter is increased. We remind the case of the  $^{48}\text{Cr}$  isotope whose deformation has been clearly established [26]. Its  $2^+$  energy is at 752 keV. Also, an energy gap at a large oblate deformation is expected at a neutron number  $N=36$ . This gap would favor oblate shape, as it is observed in  $^{74}\text{Kr}$  [27]. The  $^{60}\text{Cr}$  exhibits both a proton and neutron number associated with deformed prolate and oblate structures, respectively. There is therefore a strong -though qualitative- support for the presence of a shape coexistence in  $^{60}\text{Cr}$

$^{61}\text{V}$  and  $^{62}\text{V}$  half-lives have been measured for the first time [12]. With the very weak number of implanted nuclei in this experiment (776 and 51 for  $^{61}\text{V}$  and  $^{62}\text{V}$ ), no  $\gamma$ -line has been found in their beta-decay. A very recent experiment at GANIL has produced about 1000  $^{62}\text{V}$  using the fragmentation of a  $^{76}\text{Ge}$  beam instead of a  $^{86}\text{Kr}$  one. The strongest  $\gamma$ -line observed in its decay has an energy of 446 keV. This line can be attributed to the  $2^+$  energy of  $^{62}\text{Cr}$  (see Fig. 6). This very preliminary results, if confirmed, establishes the increase of deformation of Cr towards  $N=40$  subshell. On the basis of the low  $2^+$  energies in  $^{60,62}\text{Cr}$  and the significant drop of  $2^+$  energy in  $^{66}\text{Fe}_{40}$  [15], it is very likely that  $^{64}\text{Cr}$  would be the most deformed  $N=40$  nucleus (see below for further discussions on  $^{64}\text{Cr}$ ).

The decay curves of  $^{61-64}\text{Cr}$  extracted from [12] are presented in Fig. 3. For  $^{61-63}\text{Cr}$ , these determinations are in good agreement with those of Ameil et al. [22]. For the case of  $^{61}\text{Cr}$ , a half-life of 251(22) ms is obtained. A grow-up is present in the decay curve of  $^{62}\text{Cr}$ , which is not mentioned in. [22]. This behaviour can be explained if the half-life of the daughter nucleus  $^{62}\text{Mn}$  is shorter than that of  $^{62}\text{Cr}$ . The beta-decay of  $^{62}\text{Cr}$ , of 187(15)ms half-life, proceeds through a  $1^+$  level in  $^{62}\text{Mn}$  which subsequently  $\beta$ -decays to



$^{62}\text{Fe}$  with a half-life of 92(13)ms. It is interesting to notice that this short decay-time of  $^{62}\text{Mn}$  is in contradiction with the values of 880(150)ms and 671(5)ms measured in the decay of  $^{62}\text{Mn}$  by Runte et al. [28] and Hannawald et al. [15] respectively. This means that the beta-decay of  $^{62}\text{Cr}$  proceeds through a different state in this case. The former experiments [28,15] may favor the production of  $^{62}\text{Mn}$  in a high spin state which is not fed by  $\beta$ -decay of  $^{62}\text{Cr}$  and for which the  $\beta$  half-life is much longer. When re-analyzing their data without requiring the  $\beta$ -neutron coincidence for the determination of the half-life but only  $\beta$ -singles, a short decay-component of 84(10)ms [29] has been found on top of the long component of 671(5)ms by Hannawald et al. From the data of ref [12], a half-life of 113(16)ms has been deduced for  $^{63}\text{Cr}$ , in agreement with the value of 110(70)ms [22]. No  $\gamma$ -line has been observed far now. The  $^{64}\text{Cr}$  half-life,  $T_{1/2}=44(12)$  ms, is determined for the first time. The half-life of  $^{64}\text{Cr}$  is of importance since this nucleus lies at the  $N=40$  subshell closure.

It is interesting to apply QRPA calculations [30] with a choice of several deformations parameters to the  $\beta$ -decay of the neutron-rich  $^{63,64}\text{Cr}$  isotopes. From the “best agreement” between calculated and experimental half-lives, the deformation of nuclei can be extracted as done in [31,21,12]. The g.s. configuration of  $^{63}\text{Cr}$  is predicted to be prolate  $\epsilon_2=0.3$ , the spherical configuration being at 290 keV higher in energy. The daughter g.s. minimum is also predicted to be prolate with  $\epsilon_2=0.267$ . By using  $\epsilon_2=0.283$ , the mean value between the predicted mother and daughter deformation, the calculated  $T_{1/2}$  is 109 ms, using a  $Q_\beta$ -value of 11.16 MeV predicted by [32]. This  $Q_\beta$  is close to the prescription of Audi et al. [33] of  $11.225\pm 0.752$  MeV. The calculated value  $T_{1/2}=109$ ms is in agreement with the experimental value of  $T_{1/2}=113(16)$ ms. From this comparison, it is deduced that  $^{63}\text{Cr}_{39}$  is strongly deformed. For  $^{64}\text{Cr}$ , it is unfortunately impossible to deduce pertinent information on the deformation from these calculations since there is large discrepancy between calculated  $Q_\beta$ . Values of  $Q_\beta=8.03, 9.75$  and  $10.49$  MeV are predicted by Möller [32], Pearson et al. [34] and Audi et al. [33] respectively. As a consequence, half-lives obtained with the lower  $Q_\beta$  of 8.03 MeV are, at a given deformation parameter, about three times longer than those obtained with the  $Q_\beta$  of 10.49 MeV, keeping a fixed deformation parameter. The determination of masses in this region is therefore required in order to reduce the uncertainties on the  $Q_\beta$ -values. The differences between the mass models arise from the way authors consider or extrapolate the subshell-closure behaviour at  $N=40$ . The  $2^+$  energy of  $^{64}\text{Cr}$ , which could be obtained from the  $\beta$ -decay of  $^{64}\text{V}$  is of crucial importance to ascertain the strong deformation of  $^{64}\text{Cr}$ , which is hitherto suggested by qualitative arguments only.

## 5. Conclusions and perspectives

Experimental results aiming to study the  $N=40$  subshell via the  $\beta$ -decay of Co, Mn and V-Cr have been presented. They have brought a wealth of information on Ni, Fe, and Cr isotopes at or south to the  $N=40$  subshell closure. Complementary information from  $\mu\text{s}$ -isomers and  $\beta$ -decay isomers studies have been included to help in the assignments for these weakly produced nuclei. The presence of isomers principally originates from the  $g_{9/2}$  intruder orbital which lies right on top of the fp valence space. The implications of this intruder orbital, provided the experimental results in Coulomb excitation [5],  $\mu\text{s}$ -isomers

decay and  $\beta$ -decay studies, are at least threefolds:

- the difference in parity between fp valence space and g shell drastically reduces the possibility of making quadrupole excitations ( $2^+$  is of positive parity) across  $N=40$  in  $^{68}\text{Ni}$ . This explains both the high  $2^+$  energy of  $^{68}\text{Ni}$  and its weak  $B(E2)$  [5].

- the high pairing energy in  $g_{9/2}$  orbital as compared to  $p_{1/2}$  drastically reduces the effective strength of the energy gap at  $N=40$ , the single particle energy-gap being of the same range as pairing gap (section 2).

- for neutron-rich Cr nuclei which reside at mid- $\pi f_{7/2}$  occupancy, deformation is favoured by the combined effects of downsloping  $\pi f_{7/2}$  and  $\nu g_{9/2}$  substates as the deformation of the nucleus is increased. As a result, nuclei south to  $^{68}\text{Ni}$  are progressively deformed (sections 3,4).

The predicted strengthening of the  $N=40$  subshell-gap with the increase of isospin [1] is probably not strong enough to overcome the deformation in  $^{64}\text{Cr}$ . However only qualitative arguments supports the occurrence of a strong deformation since the  $2^+$  energy of  $^{64}\text{Cr}$  has not been determined so far, and theoretical models differ when predicting its g.s. shape ( $\epsilon_2=0$ . for [32] and  $\epsilon_2=0.257$  for [34]). In ref. [23], a deformed configuration with  $\epsilon_2=0.283$  is expected to lie only 260keV above the g.s. configuration.

With future radioactive beams facilities, one should be able to study  $^{60}\text{Ca}_{40}$  nucleus, which would be the good candidate for searching the appearance of new doubly magic nuclei arising from substantial modification of mean-field potential with large neutron-enrichment.

Acknowledgments: I wish to thank Z. Dombradi, H. Grawe, K.-L. Kratz, B. Pfeiffer and N. Vinh Mau for valuable discussions on the subjects presented in the contribution. I wish also thank my colleagues at Orsay for their permanent help during experiments and analysis of the data.

## REFERENCES

1. J. Dobaczewski et al., Phys. Rev. Lett. 72 (1994) 981.
2. R. Broda et al., Phys. Rev. Lett. 74 (1995) 868.
3. T. Pawlat et al., Nucl. Phys. A 574 (1994) 623.
4. R. Grzywacz et al., Phys. Rev. Lett. 81 (1998)
5. S. Leenhardt et al., Nuovo Cimento, 111A (1998) 733 and O. Sorlin, Fig. 6 in proceedings of the Nucleus Nucleus Conference, Strasbourg, 3rd-7th July 2000, to be published in Nucl. Phys. A.
6. A. M. Oros-Peusquens, P. F. Mantica, Nucl. Phys. A 669 (2000) 81.
7. L. Weissman et al., Phys. Rev. C59 (1999) 2004.
8. W.F. Mueller et al., Phys. Rev. Lett. 83 (1999) 3613.
9. W.F. Mueller et al., Phys. Rev. C 61 (2000) 054308.
10. U. Bosch et al., Nucl. Phys. A 447 (1988) 89.
11. J. I. Prisciandaro et al., Phys. Rev. C 60 (1999) 054307.
12. O. Sorlin et al., Nucl. Phys. A669 (2000) 351. 766.
13. S. Franchoo et al., Phys. Rev. Lett. 81 (1998) 3100.

14. M. Bernas et al., Phys. Rev. Lett. 67 (1991) 3661.
15. M. Hannawald et al., Phys. Rev. Lett. 82 (1999) 1391.
16. F. Azaiez and O. Sorlin, Nucl. Phys. News 8 91998) 34.
17. S. Raman et al. At. Data. Nucl. Data. Tables 36 (1987) 1.
18. S. Raman et al., Phys. Rev. C 37 (1988) 805.
19. S. Raman et al. Phys. Rev. C 43 (1991) 556.
20. J. M. Daugas, Phys. Lett. B 476 (2000) 213.
21. O. Sorlin et al., Nucl. Phys. A632 (1998) 205.
22. F. Ameil et al., Eur. Phys. Jour. A1 (1998) 275.
23. P. Möller, private communication.
24. H. Grawe et al., Prog. Part. Nucl. Phys. 38 (1997) 15.
25. J. I. Prisciandaro et al., contribution to the conference.
26. J. A. Cameron et al., Phys. Lett. B 387 (1996) 266.
27. C. Chandler et al., Phys. Rev. C 56 (1997) R2924.
28. E. Runte et al., Nucl. Phys. A399 (1983) 163.
29. M. Hannawald et al., Internal report from the Institut für Kernchemie 1999, Mainz.
30. P. Möller and J. Randrup, Nucl. Phys. A 514 (1990) 1.
31. O. Sorlin et al., Phys. Rev. C 47(1993)2941.
32. P. Möller, J. R. Nix and K.-L. Kratz, At. Data and Nucl. Data Tables 66 (1997) 131.
33. G. Audi, O. Bersillon, J. Blachot, A. H. Wapstra, Nucl. Phys. A 624 (1997) 1.
34. Y. Aboussir et al., At. Data and Nucl. Data Tables 61 (1995) 127.